

The spatially varying polarization of a focused Gaussian beam in quasi-phase-matched superlattice under electro-optic effect

Haibo Tang, Lixiang Chen, and Weilong She*

State Key Laboratory of Optoelectronic Materials and Technologies, Sun Yat-Sen University,
Guangzhou 510275, China
shewl@mail.sysu.edu.cn

Abstract: We present in this paper a wave coupling theory of linear electro-optic (EO) effect for quasi-phase matched (QPM) of focused Gaussian beam in an optical superlattice (OSL). The numerical results indicate that, due to the EO effect of an appropriate applied electric field, the output beam will form spatially inhomogeneous polarization, changing continuously in transverse section of beam; the confocal parameter has a significant impact on the output polarization of Gaussian beam and determines the half-wave voltage.

©2010 Optical Society of America

OCIS codes: (190.0190) Nonlinear optics; (260.5430) Polarization; (230.2090) Electro-optical devices.

References and links

1. J. Armstrong, N. Bloembergen, J. Ducuing, and P. Pershan, "Interactions between Light Waves in a Nonlinear Dielectric," *Phys. Rev.* **127**(6), 1918–1939 (1962).
2. M. Fejer, G. Magel, D. Jundt, and R. Byer, "Quasi-phase-matched Second Harmonic Generation: Tuning and Tolerances," *IEEE J. Quantum Electron.* **28**(11), 2631–2654 (1992).
3. S. N. Zhu, Y. Y. Zhu, and N. B. Ming, "Quasi-Phase-Matched Third-Harmonic Generation in a Quasi-Periodic Optical Superlattice," *Science* **278**(5339), 843–846 (1997).
4. A. Bahabad, M. Murnane, and H. Kapteyn, "Quasi-phase-matching of momentum and energy in nonlinear optical processes," *Nat. Photonics* **4**(8), 571–575 (2010).
5. Y. Lu, Z. Wan, Q. Wang, Y. Xi, and N. Ming, "Electro-optic effect of periodically poled optical superlattice LiNbO₃ and its applications," *Appl. Phys. Lett.* **77**(23), 3719–3721 (2000).
6. X. Chen, J. Shi, Y. Chen, Y. Zhu, Y. Xia, and Y. Chen, "Electro-optic Solc-type wavelength filter in periodically poled lithium niobate," *Opt. Lett.* **28**(21), 2115–2117 (2003).
7. Y. Q. Lu, M. Xiao, and G. J. Salamo, "Wide-bandwidth high-frequency electro-optic modulator based on periodically poled LiNbO₃," *Appl. Phys. Lett.* **78**(8), 1035–1037 (2001).
8. K. T. Gahagan, D. A. Scrymgeour, J. L. Casson, V. Gopalan, and J. M. Robinson, "Integrated high-power electro-optic lens and large-angle deflector," *Appl. Opt.* **40**(31), 5638–5642 (2001).
9. D. A. Scrymgeour, A. Sharan, V. Gopalan, K. T. Gahagan, J. L. Casson, R. Sander, J. M. Robinson, F. Muhammad, P. Chandramani, and F. Kiamilev, "Cascaded electro-optic scanning of laser light over large angles using domain microengineered ferroelectrics," *Appl. Phys. Lett.* **81**(17), 3140–3142 (2002).
10. V. Magni, "Optimum beams for efficient frequency mixing in crystals with second order nonlinearity," *Opt. Commun.* **184**(1-4), 245–255 (2000).
11. G. Xu, T. Ren, Y. Wang, Y. Zhu, S. Zhu, and N. Ming, "Third-harmonic generation by use of focused Gaussian beams in an optical superlattice," *J. Opt. Soc. Am. B* **20**(2), 360–365 (2003).
12. C. Zhang, Y. Q. Qin, and Y. Y. Zhu, "Perfect quasi-phase matching for the third-harmonic generation using focused Gaussian beams," *Opt. Lett.* **33**(7), 720–722 (2008).
13. L. X. Chen, and W. L. She, "Electro-optically forbidden or enhanced spin-to-orbital angular momentum conversion in a focused light beam," *Opt. Lett.* **33**(7), 696–698 (2008).
14. Q. W. Zhan, "Cylindrical vector beams: from mathematical concepts to applications," *Adv. Opt. Photon.* **1**(1), 1–57 (2009).
15. T. Brown, and Q. W. Zhan, "Introduction: unconventional polarization States of light focus issue," *Opt. Express* **18**(10), 10775–10776 (2010).
16. X. L. Wang, Y. Li, J. Chen, C. S. Guo, J. Ding, and H. T. Wang, "A new type of vector fields with hybrid states of polarization," *Opt. Express* **18**(10), 10786–10795 (2010).
17. T. van Dijk, H. F. Schouten, W. Ubachs, and T. D. Visser, "The Pancharatnam-Berry phase for non-cyclic polarization changes," *Opt. Express* **18**(10), 10796–10804 (2010).
18. M. Fridman, M. Nixon, E. Grinvald, N. Davidson, and A. A. Friesem, "Real-time measurement of unique space-variant polarizations," *Opt. Express* **18**(10), 10805–10812 (2010).

19. Y. Kozawa, and S. Sato, "Generation of a radially polarized laser beam by use of a conical Brewster prism," *Opt. Lett.* **30**(22), 3063–3065 (2005).
20. K. Yonezawa, Y. Kozawa, and S. Sato, "Generation of a radially polarized laser beam by use of the birefringence of a c-cut Nd:YVO₄ crystal," *Opt. Lett.* **31**(14), 2151–2153 (2006).
21. M. A. Ahmed, A. Voss, M. M. Vogel, and T. Graf, "Multilayer polarizing grating mirror used for the generation of radial polarization in Yb:YAG thin-disk lasers," *Opt. Lett.* **32**(22), 3272–3274 (2007).
22. H. Kawauchi, Y. Kozawa, and S. Sato, "Generation of radially polarized Ti:sapphire laser beam using a c-cut crystal," *Opt. Lett.* **33**(17), 1984–1986 (2008).
23. M. Fridman, G. Machavariani, N. Davidson, and A. A. Friesem, "Fiber lasers generating radially and azimuthally polarized light," *Appl. Phys. Lett.* **93**(19), 191104 (2008).
24. Z. Bomzon, G. Biener, V. Kleiner, and E. Hasman, "Radially and azimuthally polarized beams generated by space-variant dielectric subwavelength gratings," *Opt. Lett.* **27**(5), 285–287 (2002).
25. Q. Zhan, and J. R. Leger, "Interferometric measurement of Berry's phase in space-variant polarization manipulations," *Opt. Commun.* **213**(4-6), 241–245 (2002).
26. M. A. A. Neil, F. Massoumian, R. Juskaitis, and T. Wilson, "Method for the generation of arbitrary complex vector wave fronts," *Opt. Lett.* **27**(21), 1929–1931 (2002).
27. X. L. Wang, J. Ding, W. J. Ni, C. S. Guo, and H. T. Wang, "Generation of arbitrary vector beams with a spatial light modulator and a common path interferometric arrangement," *Opt. Lett.* **32**(24), 3549–3551 (2007).
28. G. MacHavariani, Y. Lumer, I. Moshe, A. Meir, and S. Jackel, "Spatially-variable retardation plate for efficient generation of radially and azimuthally-polarized beams," *Opt. Commun.* **281**(4), 732–738 (2008).
29. W. She, and W. Lee, "Wave coupling theory of linear electrooptic effect," *Opt. Commun.* **195**(1-4), 303–311 (2001).
30. A. Ciattoni, B. Crosignani, and P. Porto, "Optimum beams for efficient frequency mixing in crystals with second order nonlinearity," *Opt. Commun.* **177**, 9–13 (2000).
31. A. Ciattoni, G. Cincotti, and C. Palma, "Nonparaxial description of reflection and transmission at the interface between an isotropic medium and a uniaxial crystal," *J. Opt. Soc. Am. A* **19**(7), 1422–1431 (2002).
32. G. L. Zheng, H. C. Wang, and W. L. She, "Wave coupling theory of Quasi-Phase-Matched linear electro-optic effect," *Opt. Express* **14**(12), 5535–5540 (2006).
33. T. Kartaloğlu, Z. G. Figen, and O. Aytür, "Simultaneous phase matching of optical parametric oscillation and second-harmonic generation in aperiodically poled lithium niobate," *J. Opt. Soc. Am. B* **20**(2), 343–350 (2003).
34. R. Azzam, and N. Bashara, *Ellipsometry and Polarized Light* (Amsterdam: North-Holland, 1977).
35. M. V. Hobden, and J. Warner, "The temperature dependence of the refractive indices of pure lithium niobate," *Phys. Lett.* **22**(3), 243–244 (1966).
36. J. W. Zhao, C. P. Huang, Z. Q. Shen, Y. H. Liu, L. Fan, and Y. Y. Zhu, "Simultaneous harmonic generation and polarization control in an optical superlattice," *Appl. Phys. B* **99**(4), 673–677 (2010).
37. C. P. Huang, Q. J. Wang, and Y. Y. Zhu, "Cascaded frequency doubling and electro-optic coupling in a single optical superlattice," *Appl. Phys. B* **80**(6), 741–744 (2005).
38. Y. Kong, X. Chen, and Y. Xia, "Competition of frequency conversion and polarization coupling in periodically poled lithium niobate," *Appl. Phys. B* **91**(3-4), 479–482 (2008).
39. H. Tang, L. Chen, G. Zheng, D. Huang, and W. She, "Electrically controlled second harmonic generation of circular polarization in a single LiNbO₃ optical superlattice," *Appl. Phys. B* **94**(4), 661–666 (2009).
40. Z. Y. Yu, F. Xu, F. Leng, X. S. Qian, X. F. Chen, and Y. Q. Lu, "Acousto-optic tunable second harmonic generation in periodically poled LiNbO₃," *Opt. Express* **17**(14), 11965–11971 (2009).

1. Introduction

The QPM proposed by Bloembergen *et al* since 1962 [1], has become a useful technique widely used in nonlinear frequency conversions and is receiving more and more attention [2–4]. In the QPM materials, besides the second-order nonlinear optical coefficients related to frequency conversion, the EO coefficients are also periodically modulated. Therefore, the concept of QPM is also valid for the linear EO effect. Thus far, the linear EO effect based on QPM has been widely investigated, ranging from EO switch [5], precise spectral filter [6], high-frequency EO modulator [7], to EO scanner and lens [8,9]. The principles of all these devices, however, were based on the plane-wave model. As well known, the plane-wave model is valid only when the length of crystal is much shorter than the confocal parameter of light beam so that the beam width remains approximately a constant within the crystal. In fact, in the nonlinear interaction processes, especially the cascading of linear EO effect and other second-order nonlinearity effect, a focused laser beam is usually used to improve the efficiency or the signal intensity. In this case, the plane-wave model is invalid, and the transverse distribution of light field should be taken into account [10–13]. On the other hand, the formation of spatially inhomogeneous polarization beam has also attracted considerable interest [14–18]. Various methods have been proposed to form the spatially inhomogeneous polarization beam, which can be classified into two kinds: direct and indirect ones. The direct

method is by novel lasers with specially designed laser resonators [19–23]. And the indirect one is based on the wavefront reconstruction of the output field from the traditional lasers, with the aid of specially designed optical elements [16,24–28]. However, the formation of spatially inhomogeneous polarization is still a great challenge and paramount issue, due to the expectation of high flexibility in manipulating the spatially inhomogeneous polarization beam and in developing novel photonic devices and optical systems [16]. In this paper, we present a wave coupling theory of EO effect for QPM of focused Gaussian beam in an OSL. As one of its applications, the QPM-EO effect of focused Gaussian beam in a lithium niobate OSL is investigated in detail. It is found that, due to the EO effect of an appropriate applied electric field, the output beam will form spatially inhomogeneous polarization, changing continuously in transverse section of beam. And the confocal parameter has a significant impact on the output polarization of Gaussian beam and determines the half-wave voltage.

2. Theory and Analyses

Figure 1 shows the experimental schematic diagram of EO effect for QPM of focused Gaussian beam in an OSL. The applied electric field is along the y -axis of the OSL and a monochromatic light wave propagates along the x -axis of the OSL. In a cylindrical coordinate system, the total electric field participating in the process of linear EO effect can be expressed as [29]

$$\mathcal{E}(r, x, t) = \mathbf{E}(0) + [\mathbf{E}(r, x)\exp(-i\omega t)/2 + \mathbf{c.c.}], \quad (1)$$

where r is the radial distance from the propagation axis; $\mathbf{E}(0)$ is the dc electric field or slow varying electric field; $[\mathbf{E}(r, x)\exp(-i\omega t)/2 + \mathbf{c.c.}]$ is the light field with frequency ω ; $\mathbf{c.c.}$ denotes the complex conjugate. According to Ref [30,31], the paraxial approximation is determined by the parameter $g = 1/(k_0/W_0)$, where k_0 is the wave number of the light field in vacuum and W_0 is the waist radius at the input surface. For a wavelength $\lambda = 632.8$ nm, when $g = 1/(k_0/W_0) \leq 0.01$, namely $W_0 \geq 10.07 \mu\text{m}$, the paraxial approximation condition holds. And the x component (longitudinal component) of light field is too small so that it can be neglected. But, there exist two independent electromagnetic wave components of a monochromatic light wave propagating in the OSL, i.e.,

$$\mathbf{E}(r, x) = \mathbf{E}_1(r, x)\exp(ik_1x) + \mathbf{E}_2(r, x)\exp(ik_2x), \quad (2)$$

where $\mathbf{E}_1(r, x)$ and $\mathbf{E}_2(r, x)$ denote the complex amplitudes of two perpendicular components of the light field when $k_1 = k_2$, or those of two independent electric field components experiencing different refractive indices when $k_1 \neq k_2$.

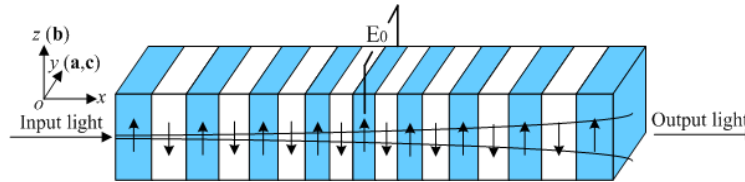


Fig. 1. The experimental schematic diagram of EO effect for QPM of focused Gaussian beam in an OSL. The arrows indicate the directions of the polarizations of crystal domains. x , y and z stand for three principal axes of the crystal. The applied electric field E_0 is along the y -axis of the OSL. \mathbf{a} , \mathbf{b} , \mathbf{c} are three unite vectors of two independent electromagnetic wave components and applied electric field, respectively.

For a Gaussian beam, the light field can be expressed as $\mathbf{E}_j(r, x) = \mathbf{G}_j(x)u_j(r, x)$ ($j = 1, 2$), where $\mathbf{G}_j(x)$ are the expansion coefficients of the Laguerre-Gaussian modes of zero order, and $u_j(r, x)$ are the Gaussian modes [10,11]. Here, the waist of the incident Gaussian beam is set at the input surface of OSL, then the two independent polarization components of light fields have the same waist radius, $W_{01} = W_{02} = W_0$. Therefore, $u_j(r, x)$ ($j = 1, 2$) read [10–12]

$$u_j(r, x) = \sqrt{\frac{2}{\pi}} \frac{1}{W_0[1-i(2x/b_j)]} \exp\left\{-\frac{r^2}{W_0^2[1-i(2x/b_j)]}\right\}, \quad (3)$$

where $b_j = k_j W_0^2$ are the confocal parameters and $b_2 = n_2/n_1 b_1$, with n_1 and n_2 being the unperturbed refractive indices of two wave components of different polarizations.

Let $\mathbf{G}_1(x) = \sqrt{\omega/n_1} A_1(x) \mathbf{a}$, $\mathbf{G}_2(x) = \sqrt{\omega/n_2} A_2(x) \mathbf{b}$, $\mathbf{E}(0) = E_0 \mathbf{c}$, where \mathbf{a} , \mathbf{b} , and \mathbf{c} are three unit vectors and $\mathbf{a} \cdot \mathbf{b} = 0$; $A_1(x)$ and $A_2(x)$ are the normalized amplitudes of the two wave components. Similarly to Ref [10–12,29,32], starting from Maxwell's equations and taking the EO second-order nonlinearity as a perturbation, we derive the wave coupling equations that describe the interaction between a light wave and an applied electric field under the slow varying amplitude approximation and the paraxial approximation, as follows

$$\begin{aligned} \frac{dA_1(x)}{dx} &= -id_1 f(x) A_2(x) \exp(i\Delta kx) \frac{1}{1+i(x/b_1)(1-n_1/n_2)} - id_2 f(x) A_1(x), \\ \frac{dA_2(x)}{dx} &= -id_3 f(x) A_1(x) \exp(-i\Delta kx) \frac{1}{1-i(x/b_1)(1-n_1/n_2)} - id_4 f(x) A_2(x), \end{aligned} \quad (4)$$

where $f(x) = 1$ and -1 correspond to the positive and negative domains of OSL, respectively;

$\Delta k = k_2 - k_1$ is the wave vector mismatch; and $d_1 = \frac{k_0}{2\sqrt{n_1 n_2}} r_{eff1} E_0$, $d_2 = \frac{k_0}{2n_1} r_{eff2} E_0$,

$d_3 = \frac{k_0}{2\sqrt{n_1 n_2}} r_{eff1} E_0$, $d_4 = \frac{k_0}{2n_2} r_{eff3} E_0$, with r_{effi} ($i = 1, 2, 3$) being the same as those in Ref.

[29].

To compensate for the wave vector mismatch perfectly, similarly to Ref [12], we consider such a structure of OSL, $f(x) = \text{sgn}(\text{Re}\{[1 + i(x/b_1)(1-n_1/n_2)]^{-1} \exp(i\Delta kx)\})$, where Re represents the real part; sgn is the sign function, $\text{sgn}(x) = 1$ when $x \geq 0$, $\text{sgn}(x) = -1$ when $x < 0$. Under the condition of QPM, Eqs. (4) can be simplified as

$$\begin{aligned} \frac{dA_1(x)}{dx} &= -id_1 A_2(x) f_1 \frac{1}{1+(x/b_1)^2(1-n_1/n_2)^2} - id_2 f(x) A_1(x), \\ \frac{dA_2(x)}{dx} &= -id_3 A_1(x) f_1 \frac{1}{1+(x/b_1)^2(1-n_1/n_2)^2} - id_4 f(x) A_2(x), \end{aligned} \quad (5)$$

where $f_1 = \int_0^L f(x) \exp[iRx + \varphi(x)] dx / L$ is the Fourier coefficient for given structure; L is the length of OSL; R is the reciprocal vector provided by the OSL; and $\varphi(x) = \arg\{[1 \pm i(x/b_1)(1-n_1/n_2)]^{-1}\}$. For plane-wave interactions, $\varphi(x)$ becomes a constant, and the OSL will degenerate to a periodic one [33].

Equations (5) are those describing the linear EO effect for QPM of focused Gaussian beam in an OSL, which are different from the coupled equations of the linear EO effect for QPM of plane-wave [32]. And the main difference is that there is a coefficient of $[1 \pm i(x/b_1)(1-n_1/n_2)]^{-1}$ for each term on the right side of Eqs. (5). The factor $[1 \pm i(x/b_1)(1-n_1/n_2)]^{-1}$ depends on x , which causes a continuously phase variation, so-called Gouy phase shift. When $x \ll b_1$, Eqs. (5) reduce to the familiar wave coupling equations under the plane-wave approximation [32].

Compared with the EO effect for QPM of the plane wave, a significant character of present case is that, due to the EO effect, the polarization of output beam will form a transversely inhomogeneous distribution in space. Generally, the description of the polarization state (ellipse) requires two parameters: azimuth angle $\psi \in [-90^\circ, 90^\circ]$ and

ellipticity $e \in [-1, 1]$ (the positive and negative correspond to right- and left-handed polarizations, respectively). ψ and e can be obtained by the relations [34]

$$\tan(2\psi) = \frac{2\text{Re}(X)}{1-|X|^2}, \quad \sin(2\arctan e) = \frac{2\text{Im}(X)}{1+|X|^2}, \quad (6)$$

where $X = E_2(r, x)/E_1(r, x) = \sqrt{\omega/n_2} A_2(x) u_2(r, x) / [\sqrt{\omega/n_1} A_1(x) u_1(r, x)]$. For a Gaussian beam, the polarization of output beam does not depend on the coordinate azimuthal angle in a cylindrical coordinate system [10–12]. However, the polarization of output beam varies with propagation distances. And more interesting is that, at a fixed x , the output beam will form a spatially inhomogeneous polarization, changing continuously in the transverse section of beam. It is obviously different from the EO effect of plane wave, for which the output beam has a polarization with homogeneous distribution transversely in space. The reason is that, two independent polarization components of Gaussian beam have different confocal parameters, i.e., $b_1 \neq b_2$, which result in a phase difference between two independent wave components in OSL. The following numerical results will illustrate this further.

In our calculation, the wavelength λ , the temperature T , the length of the OSL L and the beam waist W_0 are 632.8 nm, 298 K, 2.5 cm and 15 μm , respectively, which satisfy the paraxial approximation; the nonvanishing EO coefficients of lithium niobate used are $r_{22} = 3.4$ and $r_{51} = 3.4$ (in 10^{-12} m/V) [29]; the Sellmeier equations for lithium niobate are from Ref [35]. For an extraordinary incident beam with initial condition $A_1(0) = 0$, $A_2(0) = 1$, we obtain the numerical results shown in Fig. 2, which demonstrates the spatial distribution of polarization of output beam for different applied electric field E_0 . One sees from Figs. 2(a) and 2(e) that, when $E_0 = 0$ or 64 V/mm, the output beam is linearly polarized. This is because that when $E_0 = 0$, it has no EO effect and the output beam is an extraordinary one; and when $E_0 = 64$ V/mm,

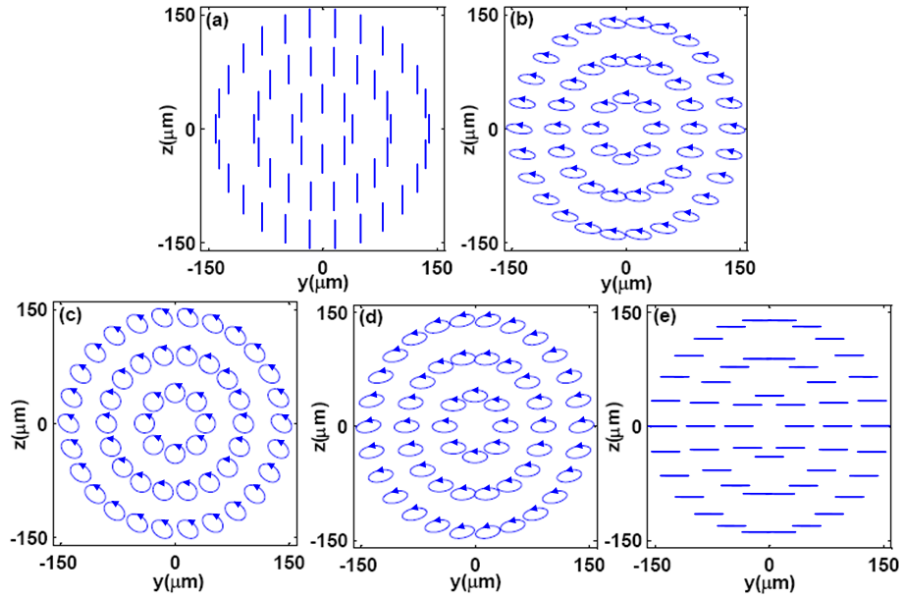


Fig. 2. The spatial distribution of polarization of output beam for different E_0 and with $\lambda = 632.8$ nm, $T = 298$ K, $L = 2.5$ cm, $W_0 = 15$ μm fixed. (a) $E_0 = 0$; (b) $E_0 = 15$ V/mm; (c) $E_0 = 30$ V/mm; (d) $E_0 = 45$ V/mm; (e) $E_0 = 64$ V/mm.

$|A_1(L)|^2 = 1$ the output beam has become an ordinary one fully. More interesting is that, when E_0 takes other values, for example, $E_0 = 15, 30$ or 45 V/mm, the polarization of output beam becomes spatially inhomogeneous. To further identify the relative change of

polarization for output beam, we plot the dependence of ψ and e on r at different E_0 , as shown in Fig. 3. One sees from Fig. 3 that, when $E_0 = 15$ V/mm [corresponding to Fig. 2(b)], ψ varies from -0.10° to -8.63° ($\Delta\psi = 8.53^\circ$) and e from -0.40 to -0.34 ($\Delta e = 0.06$) with r increasing from 0 to 150 μm ; when $E_0 = 45$ V/mm [corresponding to Fig. 2(d)], ψ varies from 0.14° to 13.82° ($\Delta\psi = 13.68^\circ$) and e from -0.48 to -0.46 ($\Delta e = 0.02$) with r (Note that in Figs. 2(b) and 2(d), though Δe are small, $\Delta\psi$ are great, the spatial inhomogeneity of polarization of output beam is still evident); and when $E_0 = 30$ V/mm [corresponding to Fig. 2(c)], ψ varies from -1.60° to -34.23° ($\Delta\psi = 32.63^\circ$) and e from -0.93 to -0.66 ($\Delta e = 0.27$) with r . Δe and $\Delta\psi$ are both great, so the spatial inhomogeneity of polarization of output beam is very evident.

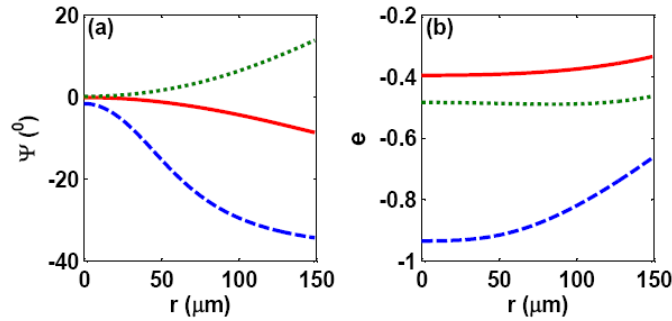


Fig. 3. Dependence of ψ and e on r for different E_0 . (a) ψ on r ; (b) e on r . Solid, long dashed, short dashed lines correspond respectively to $E_0 = 15, 30,$ and 45 V/mm for $\lambda = 632.8$ nm, $T = 298$ K, $L = 2.5$ cm, and $W_0 = 15$ μm fixed.

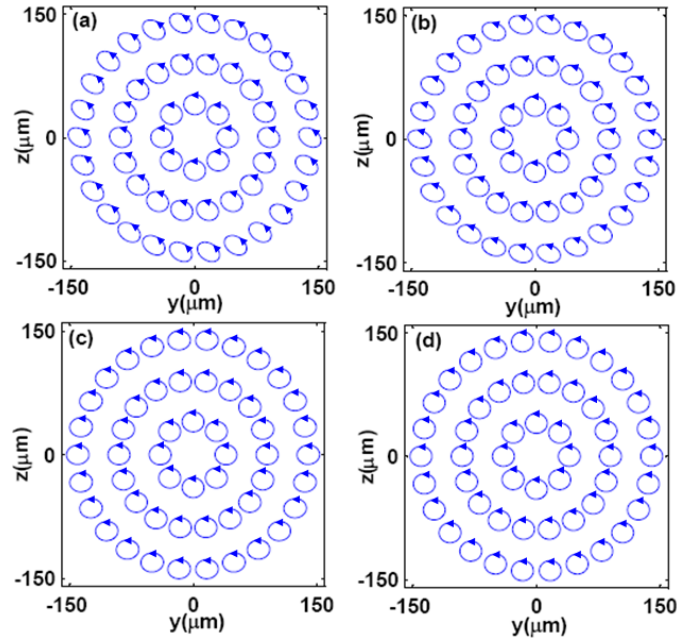


Fig. 4. The spatial distribution of polarization of output beam for different b_1 and with $\lambda = 632.8$ nm, $T = 298$ K, $L = 2.5$ cm, $E_0 = 30$ V/mm fixed. (a) $b_1 = 5.11$ mm; (b) $b_1 = 4 \times 5.11$ mm; (c) $b_1 = 16 \times 5.11$ mm; (d) $b_1 = 64 \times 5.11$ mm.

We find that the transverse spatial inhomogeneity of polarization of output beam is not only controlled by the applied electric field E_0 , but also affected by the confocal parameters b_1 and b_2 . To demonstrate this, we fix E_0 at 30 V/mm, and change b_1 ($b_2 = n_2/n_1 b_1$). The numerical results are shown in Fig. 4. It is found that, when $b_1 = 5.11$ mm ($W_0 = 15$ μm), the

spatial inhomogeneity of polarization of output beam is very evident. With the increase of b_1 , however, the transverse polarization of output beam varies gradually from spatial inhomogeneity to spatial homogeneity. It can be understood by Fig. 5. One sees that, when $b_1 = 4 \times 5.11$ mm, ψ varies from -6.62° to -20.40° ($\Delta\psi = 13.78^\circ$) and e from 0.94 to 0.68 ($\Delta e = 0.26$) with r . $\Delta\psi$ is much smaller than that at $b_1 = 5.11$ mm. And when $b_1 = 16 \times 5.11$ mm, ψ varies from -6.25° to 4.83° ($\Delta\psi = 11.08^\circ$) and e from -0.92 to -0.84 ($\Delta e = 0.08$) with r . Both of $\Delta\psi$ and Δe are much smaller than those at $b_1 = 5.11$ mm. Further, when $b_1 = 64 \times 5.11$ mm, ψ varies from -1.91° to 0.87° ($\Delta\psi = 2.78^\circ$) and e from -0.916 to -0.913 ($\Delta e = 0.003$) with r . Compared with that for $b_1 = 5.11$ mm, the $\Delta\psi$ here is very small and Δe is almost unchanged, meaning that the polarization is almost spatially homogeneous.

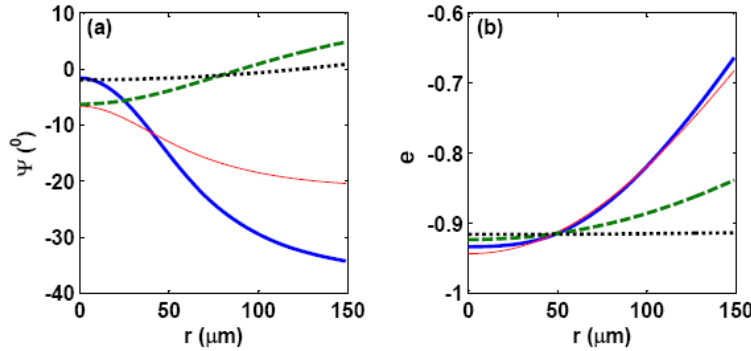


Fig. 5. Dependence of ψ and e on r for different b_1 . (a) ψ on r ; (b) e on r . Thick solid, thin solid, long dashed, short dashed lines correspond respectively to $b_1 = 5.11$, 4×5.11 , 16×5.11 , and 64×5.11 mm for $\lambda = 632.8$ nm, $T = 298$ K, and $L = 2.5$ cm fixed.

We also investigate the effect of the confocal parameter b_1 on the half-wave voltage $V_\pi = E_0'd$, where E_0' is the applied electric field for turning an extraordinary light into an ordinary one fully; d is the thickness of OSL along the direction of applied electric field. The dependence of E_0' on b_1 for the output intensity of o-ray reaching at its maximum value is shown in Fig. 6, from which one sees that, E_0' (or V_π) continually decreases as b_1 increases from 2.3 to 21.14 mm. And when $b_1 \geq 21.14$ mm, E_0' (or V_π) almost keeps a constant since $(x/b_1)^2(1-n_1/n_2)^2$ in Eq. (5) is close to zero in this case. Then, it is easy to obtain $V_\pi = (\pi\sqrt{n_1n_2}d)/(k_0r_{eff}f_1L)$ according to Ref [29,32]. The output intensity of o-ray, $|A_1(L)|^2$ as a function of b_1 and E_0 is shown in Fig. 7, which exhibits a recurrence of o-ray to its maximum intensity with E_0 for a fixed b_1 . It can be understood as follows: according to Eq. (6), the ratio $A_2(L)/A_1(L)$ determines the polarization of light field. And Fig. 7 shows that $A_1(L)$ and $A_2(L)$ have some periodicity vs E_0 for a fixed b_1 , which means that the dependence of the polarization on E_0 has some periodicity. The phenomenon is slightly different from the recent work of J.W. Zhao *et al.* [36]. In their experiment, they utilized a focused Gaussian beam to generate simultaneous second-harmonic (SH) generation (SHG) and EO coupling in a periodic or quasi-periodic OSL, where there is a competition between the SHG and EO coupling [37–39]. For a larger applied electric field, the EO coupling is dominant and the SHG becomes less efficient so that e-polarized SH becomes weak; and as a result of EO coupling, o-polarized SH also becomes weak. So for a too large applied electric field, both e- and o- polarized SH synchronously become weak, and the energy is concentrated into the fundamental wave. Therefore, the intensity of o- polarized SH does not exhibit a recurrence with E_0 . A similar mechanism was found from acousto-optic tunable SHG [40].

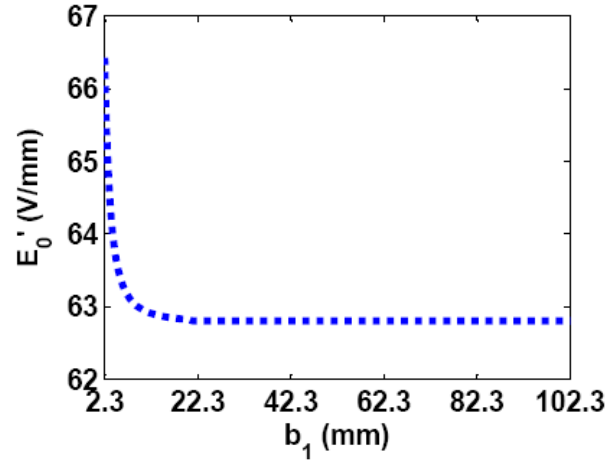


Fig. 6. Dependence of the applied electric field E_0' on the confocal parameter b_1 when the output intensity of o-ray obtains its maximum value for $\lambda = 632.8$ nm, $T = 298$ K, $L = 2.5$ cm.

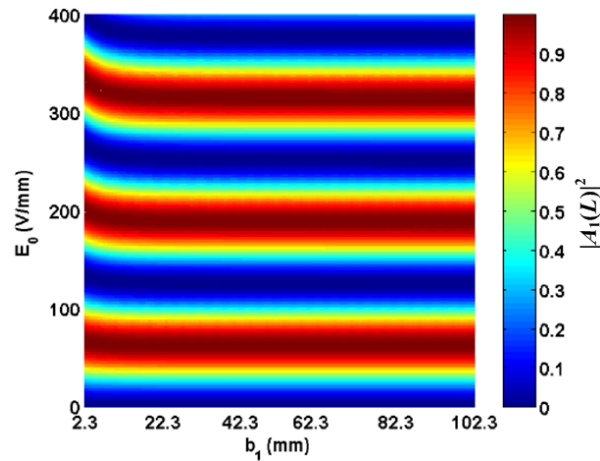


Fig. 7. The output intensity of o-ray $|A_1(L)|^2$ as a function of the confocal parameter b_1 and the applied electric field E_0 , for $\lambda = 632.8$ nm, $T = 298$ K, $L = 2.5$ cm.

3. Conclusion

In conclusion, we have developed a wave coupling theory of EO effect for QPM of focused Gaussian beam in an OSL. It is found that an electrically controllable and spatially inhomogeneous polarization beam can be obtained by a special designed OSL under EO effect. This type of spatially inhomogeneous polarization beam may have potential applications in some special photonic devices and optical systems. Here we have not considered the effects of pump-depletion, absorption, other hybrid excitation schemes and optical medium properties or defects, which are of interesting but will make the theoretical model more complicated, needing further studies.

Acknowledgments

The authors acknowledge the financial support from the National Natural Science Foundation of China (Grant No. 10874251).